Fixed-Time Adaptive Deferred Constrained Control for a Flexible Manipulator With Saturation and Variable Learning Rate

Zhijia Zhao, *Senior Member, IEEE*, Rourou Xu, Shouyan Chen, Zhijie Liu, *Member, IEEE*, Xuefeng Zhou, Keum-Shik Hong, *Life Fellow, IEEE*, and Chenguang Yang, *Fellow, IEEE*

***Abstract*—In this paper, a fixed-time adaptive deferred constrained control strategy is proposed for a flexible single-link manipulator system with input saturation. Fuzzy Neural Networks are utilized to estimate the unknown dynamics of the flexible manipulator system as well as the errors caused by input saturation. To address output constraints imposed within a prescribed time period, a time-shift function and an adjusted barrier function are introduced. The system's stability is rigorously proven using the direct Lyapunov method. Finally, numerical simulations and experimental results are presented to validate the effectiveness and superiority of the proposed control approach.**

***Note to Practitioners*—This study proposes a fixed-time adaptive deferred constrained control strategy for a flexible single-link manipulator system. The system realizes the task of enabling a flexible manipulator system with input saturation to satisfy the prescribed performance requirements at any time during operation, while achieving trajectory tracking and vibration suppression. Current research on output constraints for flexible manipulator systems primarily focuses on ensuring tracking errors converge within a preset time horizon. However, these methods assume that constraints must be applied from the very beginning, limiting the flexibility of flexible manipulator systems in real-world applications where adjustments are necessary. To address this limitation, this paper studies user-defined fixed-time output constraints and proposes an adaptive delayed control strategy. To improve convergence speed, two fuzzy neural networks with variable learning rates are integrated. Finally, simulations and experiments demonstrate the effectiveness and superiority of the proposed control approach.**

***Index Terms*—Flexible manipulator, adaptive deferred constraints control, variable learning rate, input saturation.**

Received 15 May 2025; revised 15 September 2025 and 22 October 2025; accepted 8 December 2025. Date of publication 12 December 2025; date of current version 12 January 2026. This article was recommended for publication by Associate Editor M. Labbadi and Editor H. Moon upon evaluation of the reviewers' comments. This work was supported in part by the National Natural Science Foundation of China under Grant 62273112, Grant 62473039, Grant 62433011, Grant 62403154, Grant 62473102, Grant 62573144, and Grant 62522305; in part by Guangdong Basic and Applied Basic Research Foundation under Grant 2025A1515010885, Grant 2023A1515110073, Grant 2024B1515120013, Grant 2023B1515120018, and Grant 2023B1515120019; in part by the Science and Technology Planning Project of Guangzhou, China, under Grant 2025A03J3135 and Grant 2025A04J5629; in part by the Joint Fund of Ministry of Education for Equipment Pre-Research under Grant 8091B03032303; and in part by Beijing Nova Program under Grant 20240484561. *(Corresponding authors: Shouyan Chen; Xuefeng Zhou.)*

Zhijia Zhao, Rourou Xu, and Shouyan Chen are with the School of Mechanical and Electrical Engineering and Guangdong Key Laboratory of Low-altitude Intelligent Unmanned Systems Technology for General Universities, Guangzhou University, Guangzhou 510006, China (e-mail: zhjzhaoscut@163.com; xurourou49@163.com; maxcsy@gzhu.edu.cn).

Zhijie Liu is with the Institute of Artificial Intelligence, University of Science and Technology Beijing, Beijing 100083, China, and also with Shunde Innovation School of University of Science and Technology Beijing, Foshan 528300, China (e-mail: liuzhijie2012@gmail.com).

Xuefeng Zhou is with the Institute of Intelligent Manufacturing, Guangzhou, Guangdong 510000, China (e-mail: xf.zhou@giim.ac.cn).

Keum-Shik Hong is with the School of Mechanical Engineering, Pusan National University, Busan 46241, Republic of Korea (e-mail: kshong@pusan.ac.kr).

Chenguang Yang is with the Department of Computer Science, University of Liverpool, L69 7ZX Liverpool, U.K. (e-mail: cyang@ieee.org).

Digital Object Identifier 10.1109/TASE.2025.3643613

I. Introduction

DUE to the operational demands in sectors like automotive manufacturing, production lines, and national defense, flexible manipulators have garnered widespread attention for their superior performance [1], [2]. Flexible single-link manipulator (FSLM) structures offer several advantages over rigid robotic arms, including lower weight, reduced energy consumption, and enhanced load capacity. However, the flexible structure of the manipulator may cause mechanical vibrations and deformations, worsening control performance and the device lifespan. [3], [4]. Thus, developing effective strategies for trajectory tracking and vibration suppression is essential for FSLM systems.

Over the past decade, numerous control techniques for FSLM systems have been proposed, focusing on the aforementioned issue. In [5], an optimal trajectory planning control method was proposed, addressing both trajectory tracking and vibration suppression of flexible manipulators. Nguyen and Bui, et al. proposed two models for vibration suppression and position control, with the first using two PID controllers and the second adding a fuzzy logic controller [6]. In [7], a nonlinear model of flexible manipulators using coupled duffing oscillators is developed, along with a control method to suppress their nonlinear vibrations. These studies have demonstrated effective control in trajectory tracking and vibration suppression. However, few have considered the FSLM systems with input saturation and delay constraints in this context, which constitutes the innovation of our study.

Input saturation in physical control systems occurs when the control input exceeds the actuator's maximum output capacity [8], which can negatively impact FSLM systems, leading to issues such as oscillations, tracking errors, and even potential instability. To date, many researchers have considered

input saturation in controller design [9], [10], [11]. In [9], an auxiliary variable is introduced to address the saturation nonlinearities in the uncertain Euler-Lagrange system. In [10], an anti-windup compensation method was used to address the input saturation problem in multi-agent systems. Similarly, researchers proposed a radial basis function neural network (RBFNN) controller for 2-DOF helicopter system with input saturation [11]. However, the above-mentioned literature only considered in input saturation and did not simultaneously account for both fixed-time output constraints and the effects of saturation, which motivated our research.

Given the operational demands and safety requirements of nonlinear systems, imposing output constraints is essential. Recently, numerous studies have focused on this issue. [12], [13], [14]. In [12], a prescribed performance barrier Lyapunov function was introduced to ensure the transient and steady-state performance of flexible-joint manipulator systems satisfies predefined constraints. In [13], a performance function combining prescribed performance and time consensus was used to keep the error within a predefined envelope. In [14], output constraints are managed using an exponentially decaying function. These methods help the system meet the prescribed performance requirements and ensure its stability and reliability. However, the aforementioned research approaches require that output constraints must be applied from the very beginning ($t \geq 0$).

In nonlinear systems, the initial tracking conditions are often unknown or do not need to meet specific constraints [15]. Output constraints emerge only at certain time intervals after the system has been operating, with no constraints applied during other intervals. Such constraints are typically introduced for specific purposes and are commonly encountered in practical applications. For example, a mobile robot start operating in an open space, enter a confined space after a period, and then returning to the open space. To address this situation, researchers have introduced the concept of deferred constraints [16], [17]. In [16], an adaptive Neural network (NN) algorithm was proposed for systems with delayed output constraints, ensuring the tracking error converges to a specified range within a preset time. In [17], an adaptive robust control scheme was proposed for nonlinear systems with delayed asymmetric time-varying full-state constraints, achieving trajectory tracking control. Although the aforementioned studies effectively address delayed constraints and ensure system stability and performance, the timing of output constraints implementation is not strictly predetermined, meaning the start and end times cannot be manually set. Therefore, to ensure the system output enters a specific bounded region at a precisely defined time and stays within this range for a subsequent predefined period, fixed-time control has been proposed and applied to various nonlinear systems [18], [19]. This strategy enforces stricter timing control and ensures the system achieves a stable state within the specified timeframe. Despite significant progress in many fields, no research has tackled the combined challenges of fixed-time convergence, delayed constraints, and system uncertainties in FSLM systems. In real-world scenarios of flexible manipulator systems, output constraints are often not constant throughout the process. Instead, they emerge dynamically at different time intervals as the task progresses. Consequently, developing a fixed-time deferred constraint control for FSLM system allows the system to accurately match the constraint requirements of different operational phases. This holds significant theoretical and engineering value for enhancing the system's practicality and adaptability.

NN control is an effective approach for uncertain nonlinear systems and remains an active research topic [20], [21], [22]. Fuzzy neural network (FNN) control integrates NNs with fuzzy logic systems, offering strong self-learning and self-adjusting capabilities [23]. In []

In [24], FNNs were used in complex robotic systems to handle model uncertainties and disturbances. Sun et al. developed FNN control to accurately track the desired trajectory while minimizing flexible vibrations in flexible manipulator systems [25]. In the study of flexible manipulator systems, we found that the controller's performance is significantly influenced by the learning rate of the FNN. If the NN employs a fixed learning rate (FLR), an excessively large learning rate can cause system deviations, slow convergence, or increase overshoot. Conversely, an overly small learning rate may impair the NN's ability to estimate unknown nonlinearities, degrading the overall system performance. In this field, researchers tend to adopt high-gain strategies to mitigate such effects, but this complicates the selection of controller parameters and increases the risk of controller saturation [26]. Consequently, the concept of variable learning rate (VLR) has been proposed for controller design in systems like 2-DOF helicopters [27] and robotic manipulators [28]. However, the application of NNs with VLR in FSLM systems has been scarcely explored. This provided the impetus for our research.

Inspired by the preceding analysis, this paper develops a fixed-time adaptive deferred constrained control for FSLM systems with input saturation. The principal innovations are outlined as follows

1) An effective fixed-time adaptive constrained control algorithm is proposed for FSLM systems, ensuring the tracking error converges quickly to a narrow range near zero within a fixed time. Compared with [29] and [30], the proposed control allows constraint to apply at any time interval during system operation. For instance, when the FSLM system needs to move from an open space into a constrained space for a period and then return to the open space, the control strategy can flexibly activate the constraints during the time in the constrained space to ensure safe and accurate operation, and release the constraints when back in the open space to enable more free and efficient motion. This significantly enhances the flexibility and practicality of FSLM system.
2) Unlike [31] and [32], which use RBFNNs, this study employs two FNNs to address system uncertainties and input saturation nonlinearities. Different from [25] and [33], which adopt FLR, we introduce VLRs to accelerate network convergence and enhance system performance.

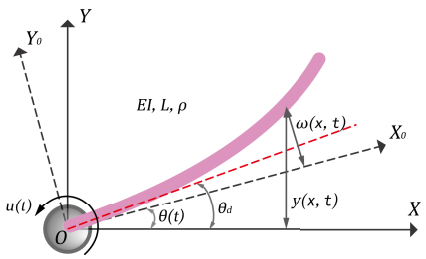

Fig. 1. Flexible single-link Manipulator.

II. Problem Statement

A. Dynamics of Flexible Single-Link Manipulator

In this article, we investigate a FSLM system equipped with boundary actuators, as shown in Fig. 1. The flexible manipulator is modeled as an Euler-Bernoulli beam of length L, positioned on a horizontal plane, with gravitational effects neglected. The inertial coordinate frame is XOY, while X_0OY_0 represents the local frame at the hub O. The beam's constant flexural rigidity is denoted by EI, and its uniform mass per unit length by ρ. The angular rotation of the hub O is represented by θ, with θ_d as its target angular rotation. Additionally, $y(x,t)$, $\omega(x,t)$, τ and I_h represent the displacement at time t, the elastic deflection of the FSLM at time t, the control torque, and the hub inertia, respectively.

Considering small-angle rotation θ, we can make the following assumption with respect to the deflection ω.

$$y(x,t) = x\theta(t) + \omega(x,t) \tag{1}$$

In this part, the dynamics of the system [34] are outlined below

$$\ddot{\omega}(x,t) + \frac{EI}{\rho}\omega''''(x,t) = -x\ddot{\theta}(t) \tag{2}$$

$$I_h\ddot{\theta}(t) = U(t) + EI\omega''(0,t) \tag{3}$$

$$\omega(0,t) = \omega'(0,t) = \omega''(L,t) = \omega'''(L,t) = 0 \tag{4}$$

In this paper, using the assumed mode method [25], the elastic deflection $\omega(x,t)$ is expressed as $\omega(x,t) = \sum_{i=1}^{N}\phi_i(x)q_i(t)$, which is a linear combination of admissible functions $\phi_i(t)$, weighted by time-varying generalized coordinates $q_i(t)$ [35]. Let $Q = \left[\theta, q, q_2, \ldots, q_N\right]^T$, the kinetic of the FSLM is $E_k = \frac{1}{2}\dot{Q}^T M_A \dot{Q}$, the potential is $E_P = \frac{1}{2}Q^T K_A Q$, and the dynamics of the FSLM can be derived through the Lagrangian equations as follows

$$M_A\ddot{Q} + K_A Q = u(t) \tag{5}$$

where $M_A \in R^{(N+1)\times(N+1)}$ is the symmetric and positive definite inertia matrix and $K_A \in R^{(N+1)\times(N+1)}$ represents the stiffness matrix of the system.

B. Input Saturation

In this paper, the effect of input saturation is taken into account. The input saturation function $u(t)$ can be expressed as follows.

$$u(v) = u(v(t)) = \begin{cases} \text{sign}(v(t))u_{\max}, & |v(t)| \geq u_{\max} \\ v(t), & |v(t)| < u_{\max} \end{cases} \tag{6}$$

where $u_{max} > 0$ is the upper bound of the saturation. It can be observed that the designed control input $v(t)$ sometimes exceeds the actual input $u(v)$. As a result, there is an error Δv between $v(t)$ and $u(v)$, and we obtain the relationship $u(v) = v(t) - \Delta v$.

C. Time-Shift Function

In this paper, to enforce output constraints only within the specified time period (T_a and T_b), and to facilitate controller design, the following time-shifting function is defined.

$$T(t) = \begin{cases} e^{-\frac{\left(\tan\left(\frac{\pi(T_a-t)}{2T_a}\right)\right)^{2m}}{2\mu_1^{2m}}}, & 0 \leq t < T_a \\ 1, & T_a \leq t < T_b \\ e^{-\frac{(t-T_b)^{2m}}{2\mu_2^{2m}}}, & t \geq T_b \end{cases} \tag{7}$$

where μ_1 and μ_2 are positive constants, and m denotes the order of the system. The following properties hold:

1) The time derivative of T is continuous for $t \geq 0$;
2) $T(t)$ increases monotonically for $0 \leq t < T_a$, and as $t \to T_a^-$, $T(T_a^-) = 1$;
3) $T = 1$ holds for $T_a \leq t < T_b$;
4) $T(t)$ decreases monotonically for $t \geq T_b$, with $T(T_b) = 1$, and $T \to 0$ as $t \to \infty$.

Let $z_1 = x_1 - x_d$, we introduce the following auxiliary variables to facilitate problem formulation.

$$\Im(t) = \begin{cases} Tz_1, & 0 \leq t < T_a \\ z_1, & T_a \leq t < T_b \\ Tz_1, & t \geq T_b \end{cases} \tag{8}$$

From (7) and (8), we can derive that for $0 \leq t < T_a$ and $t \geq T_b$, as $T \to 0$, the auxiliary function $\Im(t) \to 0$. According to the properties of $T(t)$, when $T = 0$, the system is unconstrained, and when $T = 1$, it is constrained. This allows constraints to be applied during the period from T_a to T_b after system startup.

D. Barrier Function

To address the unconstrained and prescribed output constraint problems simultaneously, a barrier function is proposed as follows

$$\xi = \frac{Q_f Q_g z_1}{\left(Q_g + \Im\right)\left(Q_f - \Im\right)} \tag{9}$$

where Q_g and Q_f are time-varying functions representing the lower and upper boundaries of z_1, respectively.

From the analysis of the denominator in (7), we find that if the the initial condition $Q_g(0) < \Im(0) < Q_f(0)$ holds, ξ remains well-defined for all $t \geq 0$. Furthermore, we observe that $\xi \to \infty$ when $\Im = -Q_g$ or $\Im = Q_f$. Thus, demonstrating that ξ is bounded for $t \geq 0$ confirms that $Q_g < \Im < Q_f$. Based on the above analysis, it can be determined that $\xi \to \infty$ occurs if and only if $z_1 \to -\frac{Q_g}{T}$ or $z_1 \to \frac{Q_f}{T}$. According to the properties of $T(t)$, during the intervals $0 \leq t < T_a$ and $t \geq T_b$, with $T \to 0^+$, we deduce that $-\infty < z_1 < +\infty$, i.e., $-\infty < x_1 - x_d < +\infty$. Thus, within this period ($0 \leq t < T_a$ and $t \geq T_b$), the system output is unconstrained ($-\infty + \underline{x}_d < x_1 < +\infty + \overline{x}_d$),

where $\underline{x}_d$ and $\overline{x}_d$ represent the minimum and maximum values of x_d, respectively. Similarly, during $T_a < t < T_b$, we have $-Q_g < z_1 < Q_f$, which implies $-Q_g + \underline{x}_d < x_1 < Q_f + \overline{x}_d$. Define $E_d = -Q_g + \underline{x}_d$ as the lower bound and $E_u = Q_f + \overline{x}_d$ as the upper bound, we conclude that the system output is constrained between E_d and E_u for $T_a < t < T_b$. Thus, the proposed fixed-time deferred constraint is feasible.

E. Fuzzy Neural Network With Variable Learning Rate

In this study, a fuzzy system is employed to manage the model uncertainties of the FSLM [36]. Consider a fuzzy system with n inputs and a single output. The l fuzzy IF-THEN rules are formulated as follows

IF x_1 is $A_1^j \ldots$ and x_n is A_n^j, THEN y is W^j, $j = 1, \ldots, N$. In addition, F^j denotes the jth rule, $1 \le j \le l$; $(x_1, x_2, \ldots, x_n)^T \in U \in U^n$ represents the input; $y \in R$ is the output; A_i^j and W^j are the fuzz sets in U and R. The degree of membership function of the FSLM is selected as

$$\mu_{A_i^j}(x_i) = \exp\left[-\frac{(x_i - c_{ij})^2}{k_{ij}^2}\right] \tag{10}$$

where $c = \left[c_1^T, c_2^T, \cdots, c_n^T\right]^T$ and k_{ij} denoting the centers and widths, respectively.

The fuzzy logic system is characterised as

$$S(x) = \frac{\sum_{j=1}^{l} y_j \left(\prod_{i=1}^{n} \mu_{A_i^j}(x_i)\right)}{\sum_{j=1}^{l} \left(\prod_{i=1}^{n} \mu_{A_i^j}(x_i)\right)}. \tag{11}$$

The FNN can approximate any unknown nonlinear function $f(Z)$ as follows

$$f(Z) = W^{*T} S(Z) + \epsilon \tag{12}$$

where Z is an input vector of the FNN, W^* is an ideal value of W, The estimated value of W^* is given by $\hat{W} = \tilde{W} + W^*$ with $\hat{W}$ denotes the estimated value of W^*, and ϵ is the approximation error constant. The fuzzy basis function vector $S(Z) = [s_1(Z), s_2(Z), \cdots, s_n(Z)]^T$.

Additionally, we introduce a Gaussian function to adjust the learning rate of the FNNs, which helps prevent rapid changes in the network weights. The weight updating laws are designed as follows

$$\dot{\hat{W}}_1 = -\Gamma\left[\phi z_2^T S_1(Z_1) + \sigma_1 \hat{W}_1\right], \phi = \phi_0 e^{-\frac{\|z_1\|^2}{\Theta^2}} \tag{13}$$

$$\dot{\hat{W}}_2 = -\Gamma\left[\phi z_2^T S_2(Z_2) + \sigma_1 \hat{W}_2\right], \phi = \phi_0 e^{-\frac{\|z_1\|^2}{\Theta^2}} \tag{14}$$

where Γ is a control gain matrices and $\sigma_1 > 0$ is an adjustable parameters. Let $W_1^{*T} S_1(Z_1) = K_A Q + M_A \dot{\alpha} - \epsilon_1(Z_1)$ and $W_2^{*T} S_2(Z_2) = \Delta v - \epsilon_2(Z_2)$, where $Z_1 = \left[Q, \dot{Q}, \alpha, \dot{\alpha}\right]^T$, $Z_2 = [v, \alpha, \dot{\alpha}]^T$.

F. Preliminaries

Lemma 1: According to Lyapunov's direct method [37], the Lyapunov candidate function $R(t)$ is bounded with an initial value $R(0)$ and satisfies $R(t) \ge 0$. Therefore, the following inequality holds.

$$\dot{R}(t) \le -\wp R(t) + \Delta \tag{15}$$

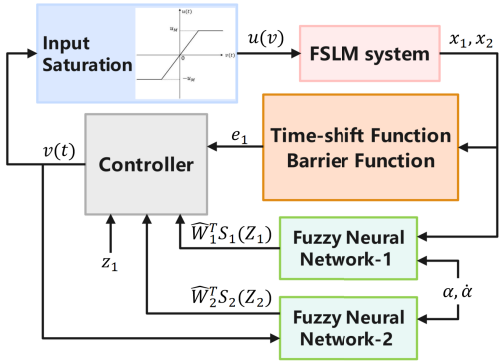

Fig. 2. The control process of the FSLM system.

where $\wp$ and Δ are positive constants.

Lemma 2: For $a, b \in R$, the following inequality holds [38].

$$ab \le \iota a^2 + \frac{1}{\iota} b^2 \tag{16}$$

where ι denotes an unknown constant.

III. Controller Design and Stability Analysis

In this section, we propose a fixed-time adaptive deferred constrained control strategy for the FSLM system with input saturation and VLR. We utilize FNNs to predict and approximate the saturation nonlinearities and the unknown system dynamics. Subsequently, Lyapunov's direct method is employed to prove system stability and ensure the tracking error converges near zero. Moreover, the system meets the prescribed performance, with vibration suppression and trajectory tracking achieved simultaneously. The control flow of the FSLM system is illustrated in Fig. 2.

As derived from (5), we set $X = [x_1, x_2]^T$, with $x_1 = Q$, $x_2 = \dot{Q}$ and $x_d = Q_d$. The desired state vector Q_d is specified as $Q_d = [\theta_d, q_{d1}, q_{d2}, \ldots, q_{dN}]^T$. Then, we define the state vectors as $z_1 = x_1 - x_d$ and $z_2 = x_2 - \alpha$, where $z_1 \in R^{(N+1)}$ and $z_2 \in R^{(N+1)}$.

The virtual controller $\alpha \in R^{(N+1)}$ is expressed as follows

$$\alpha = -\beta^{-1}(k_1 e_1 + \varepsilon \dot{T} - \psi \dot{Q}_f + \gamma \dot{Q}_g) + \dot{x}_d \tag{17}$$

where $k_1 = \mathrm{diag}(k_{11}, k_{12}, \cdots, k_{1N+1})$ is a control gain and $k_1 = k_1^T > 0, \beta = \frac{Q_g Q_f (Q_g Q_f + \Im^2)}{(Q_g + \Im)^2 (Q}, \varepsilon = -\frac{Q_g Q_f z_1^2 (Q_f - Q_g - 2\Im)}{(Q_g + \Im)^2 (Q_f - \Im)^2}, \psi = \frac{Q_g \Im z_1 (Q_g + \Im)}{(Q_g + \Im)^2 (Q_f - \Im)^2}, \gamma = \frac{Q_f \Im z_1 (Q_f - \Im)}{(Q_q + \Im)^2 (Q_f - \Im)^2}$.

By differentiating z_1 and z_2 with respect to time, we obtain

$$\dot{z}_1 = z_2 - \dot{x}_d + \alpha \tag{18}$$

$$\dot{z}_2 = M_A^{-1}[u(t) - K_A Q] - \dot{\alpha} \tag{19}$$

Define a coordinate transformation $e_1 = \xi$ and compute its derivative with respect to time as follows

$$\dot{e}_1 = \beta(e_2 + \alpha - \dot{x}_d) + \varepsilon \dot{T} - \psi \dot{Q}_f + \gamma \dot{Q}_g \tag{20}$$

The Lyapunov function candidate V_1 is formulated as $V_1 = \frac{1}{2} e_1^T e_1$. Then, taking the derivative of V_1 with respect to time and substituting (20), we get

$$\dot{V}_1 = e_1^T \beta(e_2 + \alpha - \dot{x}_d) + e_1^T(\varepsilon \dot{T} - \psi \dot{Q}_f + \gamma \dot{Q}_g) \tag{21}$$

Through the substitution of (17) into (21), the following calculation we yield

$$\dot{V}_1 = -e_1^T k_1 e_1 + e_1^T \beta z_2 \tag{22}$$

Next, the following Lyapunov function V_2 is selected as

$$V_2 = V_1 + \frac{\phi_0}{2} z_2^T M_A z_2 \tag{23}$$

After differentiating (23), substituting(19), and considering the input saturation nonlinearities, we obtain

$$\begin{aligned}\dot{V}_2 = &-e_1^T k_1 e_1 + e_1^T \beta z_2 + z_2^T \phi_0 (v(t) - \Delta v \\ &- k_A Q - M_A \dot{\alpha})\end{aligned} \tag{24}$$

To facilitate the subsequent analysis, we propose the control law $v(t)$ as follows

$$v(t) = -\frac{1}{\phi_0}\beta e_1 - k_2 z_2 + \hat{W}_1^T S_1(Z_1) + \hat{W}_2^T S_2(Z_2) \tag{25}$$

where $k_2 = \text{diag}(k_{21}, k_{22}, \cdots, k_{2N+1})$ is a control gain with $k_2 = k_2^T > 0$.

To prove the stability of the designed controller, the following Lyapunov candidate function V_3 is proposed.

$$V_3 = V_2 + \frac{1}{2}\tilde{W}_1^T \Gamma^{-1} \tilde{W}_1 + \frac{1}{2}\tilde{W}_2^T \Gamma^{-1} \tilde{W}_2 \tag{26}$$

By differentiating of V_3, approximating the unknown terms with the FNN, and substituting (13), (14) and (25), we obtain

$$\begin{aligned}\dot{V}_3 = &-e_1^T k_1 e_1 - z_2^T \phi_0 k_2 z_2 - z_2^T \phi_0 \left(1 - e^{-\frac{\|z_1\|^2}{\Theta^2}}\right) \tilde{W}_1^T S_1(Z_1) \\ &- z_2^T \phi_0 \left(1 - e^{-\frac{\|z_1\|^2}{\Theta^2}}\right) \tilde{W}_2^T S_1(Z_1) - z_2^T \phi_0 \epsilon_1(Z_1) \\ &- z_2^T \phi_0 \epsilon_2(Z_2) - \sigma_1 \tilde{W}_1^T \hat{W}_1 - \sigma_1 \tilde{W}_2^T \hat{W}_2\end{aligned} \tag{27}$$

By applying Lemma 2 and Young's inequality, and performing the calculations, we get

$$\begin{aligned}\dot{V}_3 \le &-e_1^T k_1 e_1 - z_2^T \left(\phi_0 k_2 - \frac{\Lambda(l_1 + l_2)}{2} - I\right) z_2 + \frac{1}{2}\|\epsilon_1(Z_1)\|^2 \\ &+ \left(\frac{\Lambda}{2l_1} - \frac{\sigma_1}{2}\right) \left\|\tilde{W}_1\right\|^2 + \left(\frac{\Lambda}{2l_2} - \frac{\sigma_1}{2}\right) \left\|\tilde{W}_2\right\|^2 \\ &+ \frac{\sigma_1}{2} \left\|W_1^*\right\|^2 + \frac{\sigma_1}{2} \left\|W_2^*\right\|^2 + \frac{1}{2}\|\epsilon_2(Z_2)\|^2\end{aligned} \tag{28}$$

where $\Lambda = \phi_0 \left(1 - e^{-\frac{\|z_1\|^2}{\Theta^2}}\right) \|S_1(Z_1)\|^2$ and I represents the identity matrix.

By performing the analysis and using Lemma 1, we conclude

$$\dot{V}_3(t) \le -\wp V_3(t) + \Delta \tag{29}$$

with

$$\begin{aligned}\wp = \min \Bigg\{ &2\lambda_{\min}(k_1), \frac{2\lambda_{\min}\left(\phi_0 k_2 - \frac{\Lambda(l_1+l_2)}{2} - I\right)}{\lambda_{\max}(M_A)}, \\ &\frac{\left(\frac{\Lambda}{l_1} - \sigma_1\right)}{\lambda_{\max}\left(\Gamma^{-1}\right)}, \frac{\left(\frac{\Lambda}{l_2} - \sigma_2\right)}{\lambda_{\max}\left(\Gamma^{-1}\right)} \Bigg\}\end{aligned} \tag{30}$$

$$\Delta = \frac{\sigma_1}{2} \left\|W_1^*\right\|^2 + \frac{\sigma_1}{2} \left\|W_2^*\right\|^2 + \frac{1}{2}\|\epsilon_1(Z_1)\|^2 + \frac{1}{2}\|\epsilon_2(Z_2)\|^2 \tag{31}$$

TABLE I
SIMULATION PARAMETERS OF FSLM SYSTEM

Parameter	Description	Value
L	Length of flexible link	1.0 m
EI	Bending stiffness	2.0 Nm^2
ρ	Mass per unit length	0.1 kg / m
I_h	Inertia of the hub	0.5 kgm^2

where $\lambda_{\min}(*)$ and $\lambda_{\max}(*)$ denote the smallest and largest eigenvalues of the matrix $*$, respectively.

To ensure the stability of the closed-loop system, the system parameters k_1, k_2 must satisfy the following conditions.

$$\lambda_{\min}(k_1), \lambda_{\min}\left(\phi_0 k_2 - \frac{\Lambda(l_1 + l_2)}{2} - I\right) > 0 \tag{32}$$

According to Lemma 1, the closed-loop system described in (5) can be semi-globally bounded under the proposed the fixed-time adaptive deferred constrained control.

IV. SIMULATION

In this chapter, numerical simulations verify the stability and effectiveness of the proposed control. The selected simulation parameters are shown in Table I.

The proposed control ensures that the FSLM system meet specified constraint conditions within any given time interval, while tracking the original trajectory during the remaining time intervals. Simulations were conducted based on a FSLM system with input saturation and VLR, with three cases: Case 1: $T_a = 0, T_b = 20$; Case 2: $T_a = 10, T_b = 25$; Case 3: $T_a = 0, T_b = 40$. For all three cases, the control parameters were set as $k_1 = 30I_{7\times7}, k_2 = 4I_{7\times7}, Q_f = 0.18 + 0.02\sin(t), Q_g = -0.11 + 0.025\sin(t), E_d = -0.41 - 0.025\sin(t), E_u = 0.4 + 0.02\sin(t)$and the tracking objective $x_d = 0.5(\tanh(5(t - T_a)) + \tanh(5(t - T_b)))\sin(t) + 0.3\cos(t)$.

Fig. 2 presents the simulation results for three distinct sets of time intervals (T_a, T_b): Case 1 $(T_a = 0, T_b = 20)$ is shown in panels (a) and (d); Case 2 $(T_a = 10, T_b = 25)$ is shown in panels (b) and (e); Case 3 $(T_a = 0, T_b = 40)$ is shown in panels (c) and (f). Panels (a) - (c) show the trajectory tracking responses, while panels (d) - (f) display the corresponding control input.

The following analysis can be drawn from the simulation results: For all three cases, the proposed fixed-time adaptive deferred constrained controller successfully enables the system to achieved the desired trajectory tracking, with the system output is strictly confined within within the specified range $[E_d, E_u]$ during the time interval $[T_a, T_b]$. The red curves in panels (a), (b), and (c) represent the tracking errors. In each case, the error exhibits an abrupt changes upon entering the constraint regions and then quickly converges to zero.

Taking Case 1 $(T_a = 0, T_b = 20)$ as an example in Fig. 2: As shown in panel(a), the pink curve represents the angle $\theta(t)$ which not only achieves the trajectory tracking but also stays within $[E_a, E_b]$ during the time interval $[0, 20]$. Moreover, the tracking error in panel (a), and the control input with input saturation in panel (d) both only show significant variations at $T_a = 0$ and $T_b = 20$, indicating the controller's ability

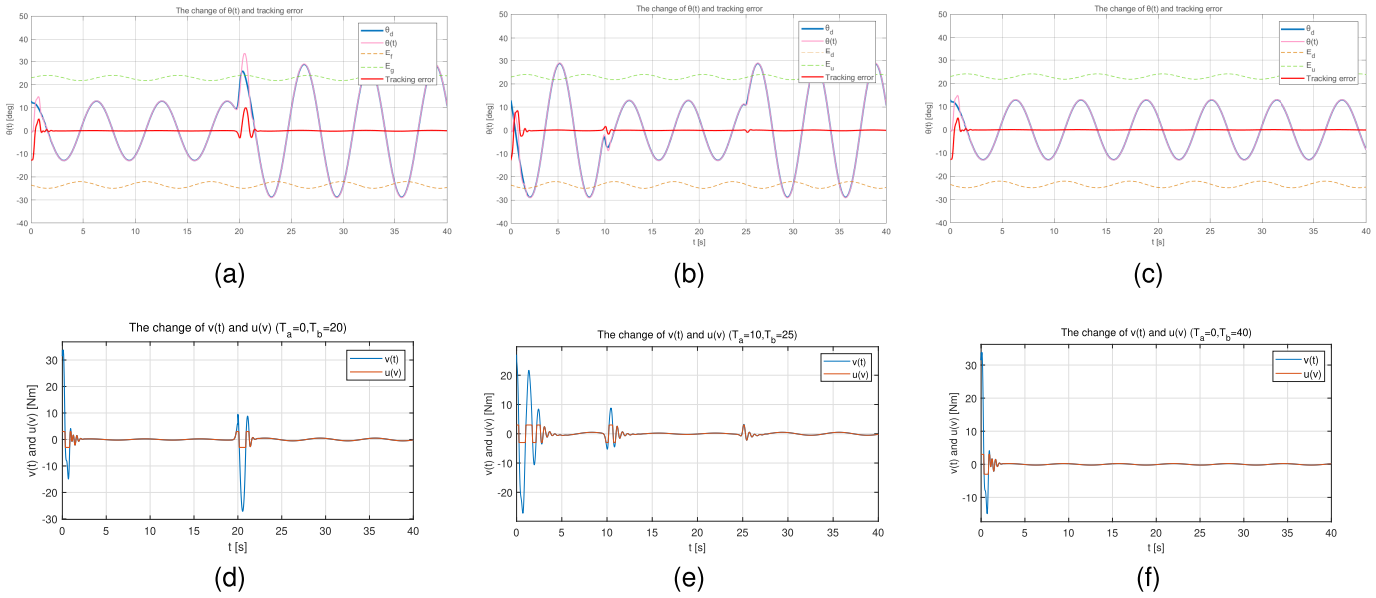

Fig. 3. Simulation results of the FSLM system under the proposed controller with three cases.

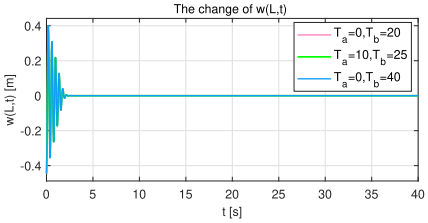

Fig. 4. The change of $\omega(L,t)$ in the simulation.

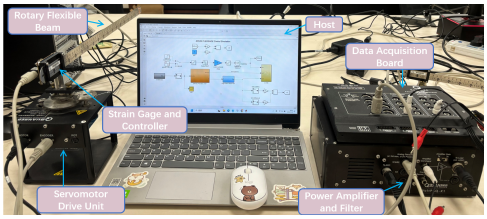

Fig. 5. Quanser experimental platform.

TABLE II
EXPERIMENT PARAMETERS OF FSLM SYSTEM

Parameter	Description	Value
L	Length of flexible link	0.419 m
EI	Bending stiffness	0.157 Nm^2
ρ	Mass per unit length	0.1 kg / m
I_h	Inertia of the hub	0.0038 kgm^2

to dynamically adapt to constraint switching without causing system oscillations

Furthermore, the vibration offset at the top $\omega(L,t)$ are presented in Fig. 3. It is evident that, since the control gains k_1 and k_2 are identical, the control law produces the same effect in terms of vibration suppression in each case. The proposed controller effectively mitigates vibration offsets and ultimately reducing the vibration offset to zero, confirming that the proposed strategy is practically effective in vibration suppression.

V. EXPERIMENT

In this chapter, three sets of experiments were conducted on the Quanser experimental platform shown in Fig. 4. Firstly, three comparative experiments are conducted by varying T_a and T_b to evaluate the proposed controller's performance under different deferred constraint requirements. Secondly, the control effects of FNNs with FLRs and VLRs are compared to analyze the impact of learning rates on the controller's performance. Finally, with $T_a = 10$ and $T_b = 25$, the proposed fixed-time adaptive deferred constrained controller was compared with the PD controller, AC, and RBFNN controller in the FSLM system with input saturation to demonstrate its superiority in handling output constraints. The selected experiment parameters are displayed in Tables II.

In the experiment, the following parameters were configured: $k_1 = 45I_{7\times7}, k_2 = 1.5I_{7\times7}, Q_f = 0.18 + 0.02\sin(t), Q_g = -0.11 + 0.025\sin(t), E_d = -0.41 - 0.025sin(t), E_u = 0.4 + 0.02\sin(t), x_d = 0.5(\tanh(5(t-T_a)) + \tanh(5(t-T_b)))\sin(t) + 0.3\cos(t)$.

A. Comparative Experiments With Different Constraint

In Fig. 5, panels (a) and (d) show the experimental results when $T_a = 0, T_b = 20$, while panels (b) and (e) correspond to the results for $T_a = 10, T_b = 25$. Panels (c) and (f) present the results when $T_a = 0, T_b = 40$. Experimental results are consistent with the simulation results, validating the effectiveness of the proposed controller in trajectory tracking. Moreover, it ensures that the output constraints remain within the range $[E_d, E_u]$ throughout any specified time interval $[T_a, T_b]$. Additionally, we can determined that the control input adjusts in accordance with the output constraint requirements for the FSLM system. Once the trajectory tracking was stabilized, the control output remains steady.

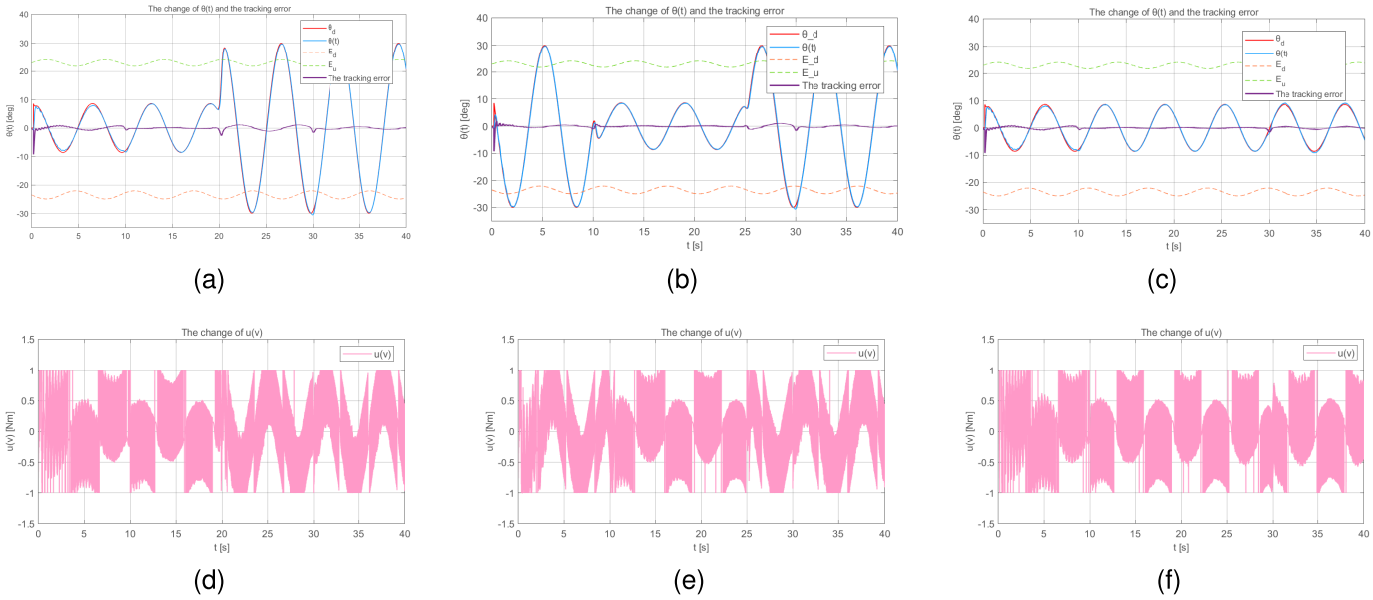

Fig. 6. Experimental results of the FSLM system under the proposed controller, with three cases (consistent with the simulation).

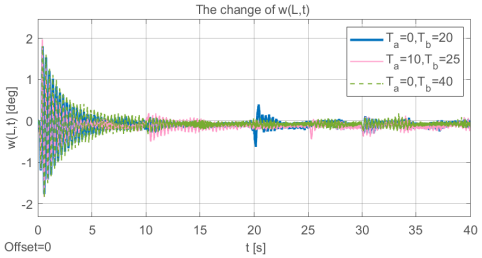

Fig. 7. The change of $\omega(L,t)$ in the experiment.

In Fig. 6, it is shown the vibration offset ω under three different cases. Experimental confirmed that the proposed controller effectively suppresses vibrations in the FSLM with input saturation. However, due to hardware limitations and external environmental factors, the experimental results are different from the simulation results. In the experiments, $\omega(L,t)$ varies across the three cases while in the simulations it remains identical.

B. Comparative Experiments With FLR and VLR

To avoid drastic changes in the NN weights at the start of system operation or when the tracking error is large, a Gaussian function is introduced into the FNN, ensuring that the network weights are adjustable. Furthermore, to demonstrate the superiority of the proposed control scheme, comparative experiments were conducted between the proposed controller with FLR and one with VLR.

As shown in Fig. 7, the plot illustrates the changes in the weights W_1 and the angle tracking results from the comparative experiment. Panels (a) shows the comparisons of W_1, under both FLR and VLR conditions.

Panels (a) can be seen that when the system begins operation with a high tracking error, the network weights in the system with VLR remain relatively low and show smaller changes. In contrast, due to its fixed and large learning rate in the system with FLR, causes the network weights to fluctuate significantly. In panels (b), the purple and pink curves respectively represent the tracking errors of the NN with VLR and FLR. It can be observed that the purple curve converges to zero more quickly than the pink curve and achieves a smaller tracking error. This suggests that introducing VLR into the NN helps to improve the system's trajectory tracking performance.

TABLE III
MAIN CONTROL LAWS OF THE COMPARATIVE CONTROLLERS

Controller	Control Law	Parameter
PD	$u(t) = -k_p(\theta - \theta_d) - k_d\dot{\theta}$	$k_p = 42, k_d = 5$
AC	$u(t) = -z_1 - k_{a2}z_2 + \hat{p}$	$k_{a1} = 20, k_{a2} = 8$
RBFNN	$u(t) = -z_1 - k_{n2}z_2 + \hat{W}^T S(Z)$	$k_{n1} = 8, k_{n2} = 3$

C. Comparative Experiments With Different Controller

As shown in Table III, the main control laws of the comparative controllers used are presented. In addition, the supplementary constants and other relevant parameters are presented as follows: in RBFNN, $\hat{W}^T S(Z) = K_A Q + M_A\dot{\alpha}, \dot{\alpha} = -k_{a1}z_1 + \dot{x}_d, \dot{\hat{W}} = -\Gamma[z_2^T S(Z) + \sigma\hat{W}], \sigma = 0.5, \Gamma = 10, c_i = 4, b_i = 1$ or -1, the number of nodes $i = 256$, in AC, $\hat{p} = K_A Q + M_A\dot{\alpha}, \dot{\hat{p}} = \gamma z_2 - \gamma\sigma\hat{p}, \gamma = 0.8, \sigma = 0.3$.

In Fig. 8, the blue, pink, yellow, and purple curves illustrate the performance of the proposed controller, the PD controller, the AC, and the RBFNN controller in tracking the desired angle. While all four controllers enable the FSLM system to achieve the target angle, their performance exhibit significant differences. The PD controller demonstrates steady-state errors during tracking and larger errors at the start of the process.The AC performs better than the PD controller but converges more slowly when approaching the constraint region. Meanwhile, the RBFNN controller exhibits pronounced tracking errors, a

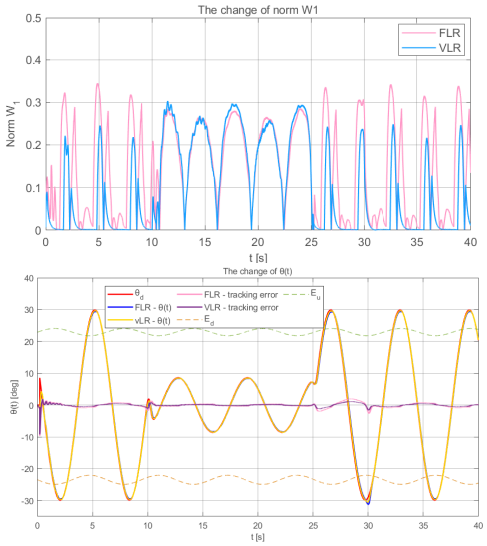

Fig. 8. Experimental results of the FSLM system under the controller with FLR and controller with VLR.

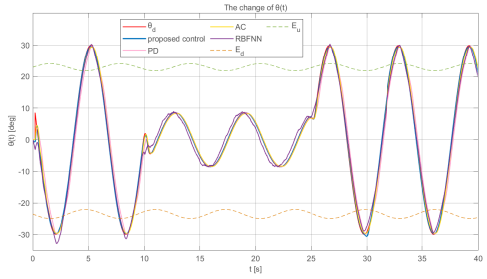

Fig. 9. Comparative experimental results of the FSLM system under the proposed controller, PD controller, AC, and RBFNN controller.

large overshoot, and significant delays throughout the process. In contrast, the proposed controller shows a clear advantage in angle tracking, with significantly reduced overshoot, superior tracking performance, and faster response speeds.

VI. Conclusion

This study presents a fixed-time adaptive deferred constrained control (25) designed to tackle the challenges of input saturation and deferred constraints. By employing the FNNs, the system's uncertainties and the errors resulting from input saturation were effectively addressed. To enhance network performance, the VLR strategy was introduced into the FNNs, which not only accelerated convergence but also prevented large fluctuations in network weights. The system's stability was rigorously proven using the Lyapunov direct method. Both simulation and experimental results confirmed that the proposed strategy effectively handles input saturation and deferred constraints. Furthermore, the experiments highlighted the advantages of VLR over FLR, demonstrating its significant contribution to system performance. While our proposed fixed-time adaptive deferred constrained control strategy has achieved certain results, its ability to ensure system robustness remains far from optimal when faced with unknown, time-varying environments and complex nonlinear conditions. In future, we will focus on addressing this issue.

References

[1] H. Wang, Z. Chen, and S. Zuo, "Flexible manipulator with low-melting-point alloy actuation and variable stiffness," *Soft Robot.*, vol. 9, no. 3, pp. 577–590, Jun. 2022.

[2] Y. Zhang, W. He, and T. Wang, "Design, modeling, and control of underwater stiffness-enhanced flexible manipulator," *Ocean Eng.*, vol. 308, Sep. 2024, Art. no. 118302.

[3] S. K. Pradhan and B. Subudhi, "Real-time adaptive control of a flexible manipulator using reinforcement learning," *IEEE Trans. Autom. Sci. Eng.*, vol. 9, no. 2, pp. 237–249, Apr. 2012.

[4] F. Cao and J. Liu, "Boundary control for PDE flexible manipulators: Accommodation to both actuator faults and sensor faults," *Asian J. Control*, vol. 24, no. 4, pp. 1700–1712, Jul. 2022.

[5] Q. Cheng, W. Xu, Z. Liu, X. Hao, and Y. Wang, "Optimal trajectory planning of the variable-stiffness flexible manipulator based on CADE algorithm for vibration reduction control," *Frontiers Bioengineering Biotechnol.*, vol. 9, Jan. 2021, Art. no. 766495.

[6] N. V. Bình and X. C. Bui, "Hybrid vibration control algorithm of a flexible manipulator system," *Robot.*, vol. 12, no. 3, p. 73, 2023.

[7] J. Huang and J. Ji, "Vibration control of coupled duffing oscillators in flexible single-link manipulators," *J. Vibrat. control*, vol. 27, nos. 17–18, pp. 2058–2068, 2020.

[8] K. Shao, J. Zheng, R. Tang, X. Li, Z. Man, and B. Liang, "Barrier function based adaptive sliding mode control for uncertain systems with input saturation," *IEEE/ASME Trans. Mechatronics*, vol. 27, no. 6, pp. 4258–4268, Dec. 2022.

[9] K. Shao, R. Tang, F. Xu, X. Wang, and J. Zheng, "Adaptive sliding mode control for uncertain Euler–Lagrange systems with input saturation," *J. Franklin Inst.*, vol. 358, no. 16, pp. 8356–8376, Oct. 2021.

[10] P. Li, F. Jabbari, and X.-M. Sun, "Containment control of multi-agent systems with input saturation and unknown leader inputs," *Automatica*, vol. 130, Aug. 2021, Art. no. 109677.

[11] J. Zhang, Y. Yang, Z. Zhao, and K. Hong, "Adaptive neural network control of a 2-DOF helicopter system with input saturation," *Int. J. Control*, vol. 21, no. 1, pp. 318–327, 2022.

[12] Y. Tuo, J. Li, and Y. Song, "Event-triggered adaptive prescribed performance control of flexible-joint manipulators with output constraint," *Eng. Comput.*, vol. 40, nos. 9–10, pp. 2432–2452, Dec. 2023.

[13] Y. Zhou, H. Yang, G. Jiang, H. Xu, J. Ying, and J. Zhang, "Prescribed-time consensus for multi-agent systems based on prescribed performance," in *Proc. 35th Chin. Control Decis. Conf. (CCDC)*, May 2023, pp. 5279–5284.

[14] Z. Liu and J. Liu, "Adaptive iterative learning boundary control of a flexible manipulator with guaranteed transient performance," *Asian J. Control*, vol. 20, no. 3, pp. 1027–1038, 2016.

[15] S. Zhou, Y. Song, and X. Luo, "Fault-tolerant tracking control with guaranteed performance for nonlinearly parameterized systems under uncertain initial conditions," *J. Franklin Inst.*, vol. 357, no. 11, pp. 6805–6823, Jul. 2020.

[16] K. Zhao, L. Chen, and C. L. P. Chen, "Event-based adaptive neural control of nonlinear systems with deferred constraint," *IEEE Trans. Syst., Man, Cybern., Syst.*, vol. 52, no. 10, pp. 6273–6282, Oct. 2022.

[17] J. Chen and C. Hua, "Adaptive full-state-constrained control of nonlinear systems with deferred constraints based on nonbarrier Lyapunov function method," *IEEE Trans. Cybern.*, vol. 52, no. 8, pp. 7634–7642, Aug. 2022.

[18] S. Cao, L. Sun, J. Jiang, and Z. Zuo, "Reinforcement learning-based fixed-time trajectory tracking control for uncertain robotic manipulators with input saturation," *IEEE Trans. Neural Netw. Learn. Syst.*, vol. 34, no. 8, pp. 4584–4595, Aug. 2021.

[19] V. Pandey, S. Kamal, and S. Ghosh, "Finite-time discrete control for two-DOF helicopter system," *IEEE Trans. Circuits Syst. II, Exp. Briefs*, vol. 71, no. 8, pp. 3800–3804, Aug. 2024.

[20] Y.-J. Liu, W. Zhao, L. Liu, D. Li, S. Tong, and C. L. P. Chen, "Adaptive neural network control for a class of nonlinear systems with function constraints on states," *IEEE Trans. Neural Netw. Learn. Syst.*, vol. 34, no. 6, pp. 2732–2741, Jun. 2023.

[21] C. Wang, L. Cui, M. Liang, J. Li, and Y. Wang, "Adaptive neural network control for a class of fractional-order nonstrict-feedback nonlinear systems with full-state constraints and input saturation," *IEEE Trans. Neural Netw. Learn. Syst.*, vol. 33, no. 11, pp. 6677–6689, Nov. 2022.

[22] H. Feng et al., "A new adaptive sliding mode controller based on the RBF neural network for an electro-hydraulic servo system," *ISA Trans.*, vol. 129, pp. 472–484, Oct. 2022.
[23] A. Bounemeur and M. Chemachema, "Adaptive fuzzy fault-tolerant control using nussbaum-type function with state-dependent actuator failures," *Neural Comput. Appl.*, vol. 33, no. 1, pp. 191–208, Jan. 2021.
[24] K. Zheng, Q. Zhang, Y. Hu, and B. Wu, "Design of fuzzy system-fuzzy neural network-backstepping control for complex robot system," *Inf. Sci.*, vol. 546, pp. 1230–1255, Feb. 2021.
[25] C. Sun, H. Gao, W. He, and Y. Yu, "Fuzzy neural network control of a flexible robotic manipulator using assumed mode method," *IEEE Trans. Neural Netw. Learn. Syst.*, vol. 29, no. 11, pp. 5214–5227, Nov. 2018.
[26] T. He and Z. Wu, "Neural network disturbance observer with extended weight matrix for spacecraft disturbance attenuation," *Aerosp. Sci. Technol.*, vol. 126, Jul. 2022, Art. no. 107572.
[27] X. Zhu, J. Shan, and I. G. G. Carmo, "Adaptive neural network control for 2-DOF helicopter with variable learning rate," in *Proc. 43rd Chin. Control Conf. (CCC)*, Jul. 2024, pp. 2306–2311.
[28] D.-D. Zheng, X. Li, X. Ren, and J. Na, "Intelligent control for robotic manipulator with adaptive learning rate and variable prescribed performance boundaries," *J. Franklin Inst.*, vol. 360, no. 11, pp. 7037–7062, Jul. 2023.
[29] X. Xing and J. Liu, "PDE model-based state-feedback control of constrained moving vehicle-mounted flexible manipulator with prescribed performance," *J. Sound Vibrat.*, vol. 441, pp. 126–151, Feb. 2019.
[30] W. Niu, L. Kong, Y. Wu, H. Huang, and W. He, "Broad learning control of a two-link flexible manipulator with prescribed performance and actuator faults," *Robotica*, vol. 41, no. 5, pp. 1371–1388, May 2023.
[31] C. He, F. Zhang, and J. Jiang, "Adaptive boundary control of flexible manipulators with parameter uncertainty based on RBF neural network," *Shock Vibrat.*, vol. 2020, pp. 1–13, Nov. 2020.
[32] Y. Ren, Z. Zhao, C. Zhang, Q. Yang, and K.-S. Hong, "Adaptive neural-network boundary control for a flexible manipulator with input constraints and model uncertainties," *IEEE Trans. Cybern.*, vol. 51, no. 10, pp. 4796–4807, Oct. 2021.
[33] W. Zhao, Y. Liu, and X. Yao, "Adaptive fuzzy containment and vibration control for multiple flexible manipulators with model uncertainties," *IEEE Trans. Fuzzy Syst.*, vol. 31, no. 4, pp. 1315–1326, Apr. 2023.
[34] X. He, S. Zhang, Y. Ouyang, and Q. Fu, "Vibration control for a flexible single-link manipulator and its application," *IET Control Theory Appl.*, vol. 14, no. 7, pp. 930–938, Apr. 2020.
[35] W. He, X. He, M. Zou, and H. Li, "PDE model-based boundary control design for a flexible robotic manipulator with input backlash," *IEEE Trans. Control Syst. Technol.*, vol. 27, no. 2, pp. 790–797, Mar. 2019.
[36] S. Qiu, Z. Li, W. He, L. Zhang, C. Yang, and C.-Y. Su, "Brain–machine interface and visual compressive sensing-based teleoperation control of an exoskeleton robot," *IEEE Trans. Fuzzy Syst.*, vol. 25, no. 1, pp. 58–69, Feb. 2017.
[37] R.-E. Precup et al., "Fuzzy logic control system stability analysis based on Lyapunov's direct method," *Int. J. Comput. Commun. Control*, vol. 4, no. 4, pp. 415–426, 2009.
[38] Y. Ren, P. Zhu, Z. Zhao, J. Yang, and T. Zou, "Adaptive fault-tolerant boundary control for a flexible string with unknown dead zone and actuator fault," *IEEE Trans. Cybern.*, vol. 52, no. 7, pp. 7084–7093, Jul. 2022.

Zhijia Zhao (Senior Member, IEEE) received the B.Eng. degree in automatic control from North China University of Water Resources and Electric Power in 2010 and the M.Eng. and Ph.D. degrees in automatic control from South China University of Technology in 2013 and 2017, respectively.

He is currently a Professor with the School of Mechanical and Electrical Engineering, Guangzhou University. His research interests include adaptive and learning control, flexible mechanical systems, ocean cybernetics, and robotics.

Dr. Zhao has been an Associate Editor of IEEE TRANSACTIONS ON AUTOMATION SCIENCE AND ENGINEERING, IEEE TRANSACTIONS ON NEURAL NETWORKS AND LEARNING SYSTEMS, IEEE TRANSACTIONS ON SYSTEMS, MAN, AND CYBERNETICS: SYSTEMS and other flagship journals.

Rourou Xu received the B.Eng. degree in robotics engineering from the School of Mechanical and Electrical Engineering, Guangzhou University, Guangzhou, China, in 2023, where she is currently pursuing the M.E. degree of control engineering.

Her current research interests include adaptive control, neural network control, flexible mechanical intelligent control systems, and robotics.

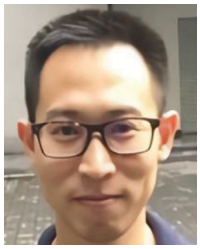

Shouyan Chen received the B.Eng. degree in process control and the Ph.D. degree in robotic dynamics and control from South China University of Technology, Guangzhou, China, in 2008 and 2017, respectively.

He is currently an Associate Professor with the School of Mechanical and Electrical Engineering, Guangzhou University, Guangzhou. His research interests include robotics, human–robot interaction, and intelligent control.

Zhijie Liu (Member, IEEE) received the B.Sc. degree from China University of Mining and Technology (Beijing), Beijing, China, in 2014, and the Ph.D. degree from Beihang University, Beijing, in 2019.

In 2017, he was a Research Assistant with the Department of Electrical Engineering, University of Notre Dame, for twelve months. He is currently a Full Professor with the School of Intelligence Science and Technology, University of Science and Technology Beijing, Beijing. His research interests include adaptive control, modeling and vibration control for flexible structures, and distributed parameter systems.

Xuefeng Zhou received the M.E. and Ph.D. degrees in mechanical engineering from South China University of Technology, Guangzhou, China, in 2006 and 2011, respectively.

He is currently the Deputy Director of the Institute of Intelligent Manufacturing, Guangdong Academy of Sciences, Guangzhou. His research interests include robot learning and robotized intelligent manufacturing.

Keum-Shik Hong (Life Fellow, IEEE) received the B.S. degree in mechanical design from Seoul National University in 1979, the M.S. degree in mechanical engineering from Columbia University, New York, in 1987, and the M.S. degree in applied mathematics and the Ph.D. degree in mechanical engineering from the University of Illinois Urbana–Champaign, Champaign, IL, USA, in 1991.

In 1993, he joined the School of Mechanical Engineering, Pusan National University. His research interests include brain–computer interface, nonlinear systems theory, adaptive control, and distributed parameter systems. He is a fellow of Korean Academy of Science and Technology, an ICROS Fellow, and a member of the National Academy of Engineering of Korea. He has received many awards, including the Best Paper Award from the KFSTS of Korea in 1999 and the Presidential Award of Korea in 2007. He served as an Associate Editor for *Automatica* from 2000 to 2006, the Editor-in-Chief for *Journal of Mechanical Science and Technology* from 2008 to 2011, and the Editor-in-Chief for *International Journal of Control, Automation, and Systems*. He was the President of the Institute of Control, Robotics, and Systems (ICROS), South Korea, and Asian Control Association.

Chenguang Yang (Fellow, IEEE) received the B.Eng. degree in measurement and control from Northwestern Polytechnical University, Xi'an, China, in 2005, and the Ph.D. degree in control engineering from the National University of Singapore, Singapore, in 2010.

He performed postdoctoral studies in human–robotics with Imperial College London, London, U.K, from 2009 to 2010. His research interest include human–robot interaction and intelligent system design. He is currently the Chair in robotics with the Department of Computer Science, University of Liverpool, U.K. He was awarded U.K. EPSRC UKRI Innovation Fellowship and individual EU Marie Curie International Incoming Fellowship. As the lead author, he received IEEE TRANSACTIONS ON ROBOTICS Best Paper Award in 2012 and IEEE TRANSACTIONS ON NEURAL NETWORKS AND LEARNING SYSTEMS Outstanding Paper Award in 2022. He is the Corresponding Co-Chair of the IEEE Technical Committee on Collaborative Automation for Flexible Manufacturing.